J Mater Sci: Mater Med (2014) 25:1875–1884
DOI 10.1007/s10856-014-5232-2

Controlled oxidative nanopatterning of microrough titanium surfaces for improving osteogenic activity

Guoxin Tan · Ying Tan · Guoxin Ni · Guobo Lan · Lei Zhou · Peng Yu · Jingwen Liao · Yu Zhang · Zhaoyi Yin · Hang Wang · Chengyun Ning

Received: 24 January 2014 / Accepted: 29 April 2014 / Published online: 15 May 2014

Abstract To further enhance the biological properties of acid-etched microrough titanium surfaces, titania nanotextured thin films were produced by simple chemical oxidation, without significantly altering the existing topographical and roughness features. The nanotextured layers on titanium surfaces can be controllably varied by tuning the oxidation duration time. The oxidation treatment significantly reduced water contact angles and increased the surface energy compared to the surfaces prior to oxidation. The murine bone marrow stromal cells (BMSCs) were used to evaluate the bioactivity. In comparison, oxidative nanopatterning of microrough titanium surfaces led to improved attachment and proliferation of BMSCs. The rate of osteoblastic differentiation was also represented by the increased levels of alkaline phosphatase activity and mineral deposition. These data indicated that oxidative nanopatterning enhanced the biological properties of the microrough titanium surfaces by modulating their surface chemistry and nanotopography. Based on the proven mechanical interlocking ability of microtopographies, enhancement of multiple osteoblast functions attained by this oxidative nanopatterning is expected to lead to better implant osseointegration in vivo.

Electronic supplementary material The online version of this article (doi:10.1007/s10856-014-5232-2) contains supplementary material, which is available to authorized users.

G. Tan (✉) · Y. Tan · L. Zhou · H. Wang
School of Chemical Engineering and Light Industry, Guangdong University of Technology, Guangzhou 510006, China
e-mail: tanguoxin@126.com

G. Ni · G. Lan
Department of Orthopaedics and Traumatology, Nanfang Hospital, Southern Medical University, Guangzhou 510515, China

P. Yu · J. Liao · C. Ning (✉)
College of Materials Science and Technology, South China University of Technology, Guangzhou 510641, China
e-mail: imcyning@scut.edu.cn

Y. Zhang
Hospital of Orthopaedics, Guangzhou General Hospital of Guangzhou Military Command, Guangzhou 510010, China

Z. Yin
School of Material Science and Engineering, Kunming University of Science and Technology, Kunming 650093, China

1 Introduction

Titanium is extensively used as load-bearing implants due to its excellent biocompatibility and high mechanical strength [1]. However, the host tissue response to titanium implant is not always favorable due to its bioinert nature with a native oxide layer. It is well-established that the synthetic titanium oxide layer cannot only enhance the potential resistance to corrosion [2] but also improve implant bioactivity [3]. Therefore, it is desirable for titanium implants to form a compact and homogeneous titanium oxide layer on the metal surface through surface modification techniques.

Besides surface chemistry, surface topography also plays an important role in deciding the bone-titanium integration. Since bone tissues are composed of nanostructures including non-collagenous organic proteins, fibrillar collagen and hydroxyapatite crystals, nanopatterning technology is expected to offer biologically optimized surfaces for implantable materials. In fact, considerable biological evidence has been established for the efficacy of titanium implants with nanostructured

surface created by several methods such as chemical treatment, anodic oxidation and electron-beam lithography [4–6]. For instance, the adhesion, proliferation and osteogenic differentiation were promoted on titanium surfaces with a nano-sawtooth structures compared with relatively smooth titanium surfaces [7]. The titania nanotubes with bigger dimensions had higher interaction energies, and thus leading to higher protein adsorption and obvious influences on cell behaviors [8]. Another advantage of the nanopatterning technology would be the potential capability of forming nanostructures on microrough surfaces with preserving the existing morphology, which may be used to provide additional or synergistic functionalization of nanostructures with the benefits of existing microstructures. There are reports demonstrating the good cell behaviors on these kinds of hierarchical structured materials surface. Zhao et al. [9] developed a micro–nano textured hybrid titanium surface with titania nanotubes by simple acid etching followed by anodization, which led to enhancement of multiple osteoblast functions. Ueno et al. [10] introduced nanopolymorphic features to microrough titanium surfaces by a combination of sandblasting and alkali-and heat-treatment and these surfaces significantly increased the implant fixation and the percentage of bone-implant contact. Despite some promising results have been reported, it is still challenging to develop effective methods for creating hybrid micro–nano textured structures that can be directly used in clinic.

Chemical oxidation based on mixtures containing aqueous hydrogen peroxide (H_2O_2) has been demonstrated to be a versatile way to create reproducible nanopatterns on pure Ti and Ti alloy and allow significantly enhanced cellular response [11]. Besides, varying the acidic (or basic) component in mixtures containing H_2O_2 appreciably changed the nanostructure on Ti surfaces, which have been demonstrated to exert different influence on the behavior of various cell types [12]. However, very limited work has focused on utilizing this oxidative patterning to superimpose nanotextures onto microtopography, even though previous study has revealed its possibility of modulating the microtopography of titanium surface [13]. In this paper, micro–nano-hybrid architectures were created by acid etching titanium surfaces followed by controlled oxidizing in a H_2SO_4/H_2O_2 mixture. Tuning the oxidation duration time revealed to change the nanopatterns on microrough titanium surfaces and smear the existing micro-texture to different extent. Murine bone marrow stromal cells (BMSCs) were used to probe the additional effect of the oxidized nanostructures on both initial and subsequent osteogenic events. We hypothesized that the change in the surface chemistry and nanotopography of microrough titanium surfaces would prospectively enhance their biological properties.

2 Materials and methods

2.1 Controlled chemical oxidation of Ti disks

Pieces of the substrates of 10 × 0.1 mm (diameter × thickness) in size were cut from a sheet of biomedical pure titanium, which were obtained according to standard ASTM (American Society for Testing & Materials) F67-2000 from Baoji Qichen New Material Technology Co., Ltd. Titanium substrates were ultrasonically cleaned with acetone, alcohol and distilled water separately for 10 min. After being dried in air, samples were etched for 5 min in a mixture of HF, HNO_3 and distilled water. These acid-etched samples were set as control and designated as "pure Ti" (pTi). The reaction solution used for oxidizing was prepared by carefully adding concentrated H_2SO_4 (98 %, sigma) to 30 % aqueous H_2O_2 (sigma) in the ratio 7:3. The acid-etched titanium substrates were immersed in the fresh aforementioned solution at 60 °C for 10, 30 and 90 min, and denoted as the Ti-10, Ti-30 and Ti-90 samples, respectively. The oxidized samples were thoroughly rinsed with deionized water and air-dried.

2.2 Surface characterization

The surface morphology was examined with a field emission scanning electron microscopy (Nova NanoSEM430, FEI, Netherlands). Surface roughness measurements of samples were made using atomic force microscopy observations (SPM-9600, SHIMADZU, Japan) over 10 × 10 μm and 500 nm × 500 nm area. The chemical structures of the titanium and oxygen atoms on the surface were analyzed by XPS (ESCALAB 250, Thermo-VG Scientific,America). Their spectra were curve-fitted using a computer-assisted Lorentzian–Gaussian peak model. The binding energy of the C1s line at 284.5 eV was taken as a reference peak for calibrating the obtained spectra. The crystalline phases of the film were studied by X-ray diffractometry (D8 ADVANCE, Bruker, German) operated under the conditions of 40 kV and 40 mA, equipped with a thin-film attachment on which the glancing angle was fixed at 1°.

2.3 Contact angle measurement for surface energy

The wettability of the samples was determined by the sessile-drop contact angle method using a contact angle meter (DIGIDROP, Zeiss, German). To obtain the total surface energy and its polar/dispersive components, two solvents, i.e. di-iodomethane and ultrapure water, were applied. Contact angles for each solvent were measured at 5 s after placing the drop (1 μL drops) at 25 °C and repeated with five drops. The surface energies were calculated using the Owens–Wendt–Kaeble's equation:

$$r_L(1 + \cos\theta) = 2\left(r_S^d r_L^d\right)^{1/2} + 2\left(r_S^p r_L^p\right)^{1/2} \quad (1)$$

where, r_L and r_S are the liquid surface tension and solid surface energy, respectively. The final surface energy (r_s) is equal to the sum of its dispersion (r_S^d) and polar (r_S^p) components.

2.4 Cell culture

Murine BMSCs were purchased from ATCC (NO. CRL-12424). The cells of passage 3–4 were used in the experiments. For adhesion, proliferation and morphology observation analysis, cells were cultured in Dulbecco's modified Eagle's medium (DMEM) supplemented with 10 % fetal bovine serum (FBS) in a humidified atmosphere of 5 % CO_2 at 37 °C. For differentiation study, the medium was supplemented with 10 mM Na-β-glycerophosphate, 50 μg/ml ascorbic acid and 10^{-8} M dexamethasone. The medium was replaced every two days. The pTi and Ti-30 samples were placed in 48 well plates and the BMSCs were seeded at a density of 10,000 cells/well for all experiments.

2.5 Cell adhesion and proliferation assay

Cell adhesion was investigated using a commercially available live/dead assay. After cultivation for 24 h, the living and dead cells were, respectively, stained with Calcein-AM and Ethidium homodimer (Sigma) for 30 min at 37 °C, and then visualized using a fluorescence microscope (Olympus, 1X2-ILL 100, Japan). Additional cell proliferation was quantified. At predetermined time intervals (1, 3 and 5 days), specimens were rinsed with PBS and CCK-8 proliferation kit reagents were added to the specimens. After 1 h incubation, reagents were carefully transferred to 96-well plates. The optical density was measured using a microplate reader (Thermo Scientific, Multiscan GO, USA) at a wavelength of 450 nm.

2.6 Cell morphology observation

After 24 h of culture, cells attached to the disks were sequentially fixed with 2 % glutaraldehyde and 1 % osmiumtetroxide and dehydrated using an ascending series of alcohols. After critical point drying and gold coating, the morphologies of the cells on titanium surfaces were observed using SEM.

2.7 Alkaline phosphatase activity and mineralization assay

The alkaline phosphate (ALP) activity was measured by an assay based on the hydrolysis of p-nitrophenyl phosphate (p-NPP) (Sigma-Aldrich, UK) to p-nitrophenol (p-NP) in the presence of ALP. After cultivation for 4, 7 and 14 days respectively, the production of pNP was determined by the absorbance at 405 nm measured using a microplate reader. The mineralization by the cells was examined by Alizarin Red S staining. After 14 days of incubation, the cells were washed three times with PBS and then fixed with 75 % ethanol for 1 h. The samples were stained using 1 % Alizarin Red S solution for 5 min and finally washed with distilled water. Images of stained surfaces were captured by a digital camera (NikonD3200, Japan). For quantification of Alizarin Red S, the stained samples were desorbed using 10 % cetylpyridinium chloride (Sigma), and the OD values for absorbance of the eluent were determined at 620 nm.

2.8 Statistical analysis

The data were collected from four separate experiments and expressed as mean ± standard deviation. The one-way ANOVA is employed to test the significance of treatment effects on cell proliferation and differentiation, where the ANOVA is implemented using the SPSS 15 statistical system (SPSS Inc., Chicago IL, USA). Values of $P < 0.05$ were considered statistically significant.

3 Results and discussion

3.1 Surface topography

To determine the distributions of nanofeatures on titanium surfaces with different oxidization time, disks were observed by SEM. Images of low magnification (see Online Resource Fig. S1) showed that acid-etched surfaces after 0, 10 and 30 min of oxidation showed a very similar microscale stepped-morphology, ranging 0.2–3.0 μm in edge-to-edge distance (approximately 1 μm on average). After 90 min of oxidation, the original stepped-morphology disappeared and the intergranular corrosion became prominent, just the same as in [14], which was caused by the higher chemical reactivity of grain boundary than that of the grain interior. High-resolution SEM imaging reveals more details of surfaces (Fig. 1). Nanosheets-like structures (Fig. 1a) were sparsely distributed on the acid-etched microtopography. After subsequent oxidization, the sharp edges were smoothed and different novel nanopatterns formed on titanium surfaces. When subjected to the oxidation for 10 min (Fig. 1b), the surface revealed a network characterized by nanopitting. As shown in Fig. 1c, nanopits were not clearly distinguishable and mesoporous patterns were presented after 30 min of reaction. For a prolonged duration of oxidation, i.e. 90 min, the entire surface was covered by a nanotip-like structure (Fig. 1d). These results

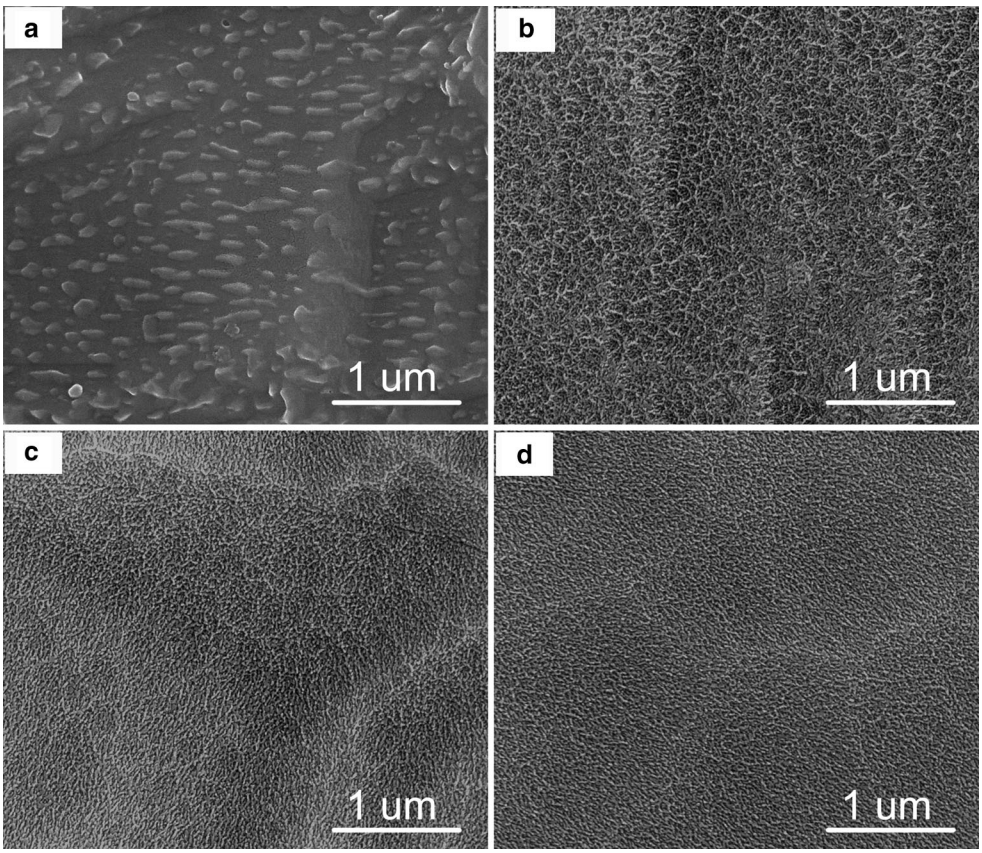

Fig. 1 SEM images (×80,000) of acid-etched titanium surfaces oxidized by H_2SO_4/H_2O_2 solution for 0 min (**a**), 10 min (**b**), 30 min (**c**) and 90 min (**d**), respectively

clearly indicated that micro–nano-hybrid architecture can be created on titanium surface by controlling the processing time. No exfoliation of layer after sonication confirmed the stability of nanofeatures created in our short-time oxidation. The nanopatterns obtained in our results were different with the typical sponge-like structure reported by previous report [15], which might be due to the difference both in the pretreatment and the processing temperature. Variola [14] found titanium oxide thickness increased with the extension of etching time in the H_2SO_4/H_2O_2 mixture until it reached a maximum value. Obviously, this conclusion was also applicable to our results.

AFM images of the acid-etched titanium surfaces before and after oxidation were presented in Fig. 2. Low-magnification images (10 μm × 10 μm) showed that oxidization for 30 min or less did not significantly affect the original micro-scale stepped-morphology, which might promote bone-to-implant contact via such mechanisms as mechanical interlocking [16]. However, the acid-etched surface after 90 min of oxidation showed a significant change in morphology. The sharp ridges of micro-stepped structures became blurry, which was due to the "smoothening" effect brought about by chemical dissolution. Surface topography quantification based on 10 μm × 10 μm AFM images showed an irregular reduction in roughness values in relation to the reaction time. This might be caused by the non-homogeneous distribution of the irregular micro-stepped morphology. At high magnification (500 nm × 500 nm), the pTi sample showed a comparatively smooth morphology at the nanometer scale, and traces related to acid treatment were the only features observed. Instead, the oxidative treatment produced morphologies with ultrafine nanofeatures. The nanofeatures were not consistent with the results of SEM, which might be relevant to the technology employed. Rani et al. [17] have demonstrated that different non-periodic nanostructures, such as nanoscaffold, nanoleaf, nanoneedle, developed on titanium implants helped to improve bone integration. Therefore, it was reasonable to speculate that the nanopatterns added on the microrough titanium surface in our study would favor positive interaction with cells.

3.2 Surface wettability and surface energy

The wettability of the surface, indicative of surface energy, plays an important role in protein adsorption, cell attachment and spreading [18, 19]. The variation in contact angles of titanium surfaces was shown in Fig. 3a for different test liquids. Static water contact angle for titanium surfaces reduced

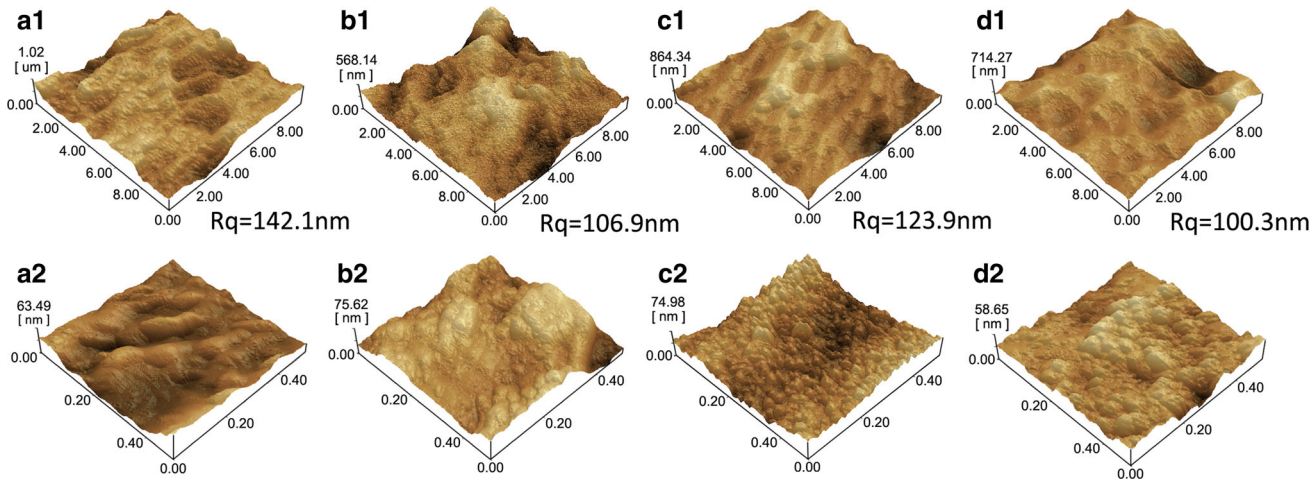

Fig. 2 AFM topographies of acid-etched titanium surfaces oxidized by H_2SO_4/H_2O_2 solution for 0 min (**a1**, **a2**), 10 min (**b1**, **b2**), 30 min (**c1**, **c2**) and 90 min (**d1**, **d2**) respectively. Pictures of 10 μm × 10 μm (*top*) show the morphology of overall view and higher magnification of 500 nm × 500 nm (*bottom*) displays the detail of nanostructured surfaces

from 97.5 ± 3.0° to 13.3 ± 4.4° for first 10 min of exposure time, indicating that the modification process greatly increased surface wettability. The values did not change significantly with longer exposure time, and even slightly higher values were observed up to 18.2 ± 5.1° and 23.2 ± 6.4° for Ti-30 and Ti-90 samples respectively. Surface energies of titanium samples calculated from the contact angles using Eq. (1) were shown in Fig. 3b with their polar and dispersive components. It can be seen that all modified samples showed a dramatic increase in total surface energy. The increase in surface energy was mainly attributed to its polar component, which indicates the possibility of introduction of polar groups onto the surface. In the present study, oxidative nanopatterning could remove possible adsorbates which are typically present on acid-etched samples and introduce hydroxyl groups on titanium surfaces, thus leading to improved hydrophilicity and higher surface energy. Besides, the influence of surface roughness on the wettability of a solid has been proposed. According to the Wenzel approach [20], an increase in the surface roughness should lead to a decrease in the values of contact angles for hydrophilic surfaces due to the increase in surface area. Therefore, the higher surface energy of oxidized samples might partly be caused by their increased surface area. The role of surface energy in regulating cell response to implant surfaces has been studied [21]. In general, higher surface energy is able to enhance the early cellular response at the cell-implant interface by adsorbing more proteins, promoting cell adhesion and spreading [22].

3.3 Surface composition

Chemistry of substrate is an important factor influencing the osteoblast responses [23]. In our study, the surface composition of nanostructured titanium surfaces was not significantly affected by the oxidative treatment. In order to have a sight into the change of surface chemistry before and after oxidation, Ti2p and O1 s high-resolution XPS spectra (Fig. 4) of pTi and Ti-30 sample were compared. As shown in Fig. 4a,c, a characteristic doublet peak located at 459.0 and 464.7 eV is attributed to Ti^{4+}, showing that TiO_2 is the main component of both oxide layers. Deconvolution of the pTi spectrum revealed the presence of Ti^{3+} (457.4 and 464.2 eV) and Ti^{metal} (454.1 and 460.2 eV), which presumably arise, respectively, from Ti_2O_3 and the underlying Ti substrate [15]. Only an intense Ti^{4+} doublet was detected and suboxides could no longer be observed on Ti-30, demonstrating that the oxide layer consists of pure TiO_2 after 30 min oxidation. Moreover, the disappearance of Ti^{metal} peak in Ti-30 was due to the titania layer formation, which might be able to act as a diffusion barrier for preventing or minimizing toxic ion release from the metal substrates [24], improving the long-term biocompatibility of metals. We also compared changes in the O1s region between pTi and Ti-30 samples. Fig. 4b,d shows main peaks close to 530.1 eV and broadenings at 531.5 and 532.7 eV for both samples, corresponding, respectively, to the binding energies of atoms involved in Ti–O bonds, OH groups, and adsorbed H_2O. In comparison with the amorphous TiO_2 phase or rutile, the anatase phase of titania has been reported to exhibit better biocompatibility [25]. Typical diffraction peaks corresponding to metallic titanium (at 40.5° and 53.2°) with (101) and (102) reflections were present in both XRD patterns (shown in Online Resource Fig. S2). After oxidization, the diffraction peaks from the metal substrates were suppressed, as sign of the increase thickness of the oxide layer. None characteristic peak of either anatase or rutile phases of TiO_2 was detected, indicating that the oxidative nanopatterning process did not alter the amorphous nature of the native TiO_2 layer. With no need of subsequent calcinations or hot water aging, chemical

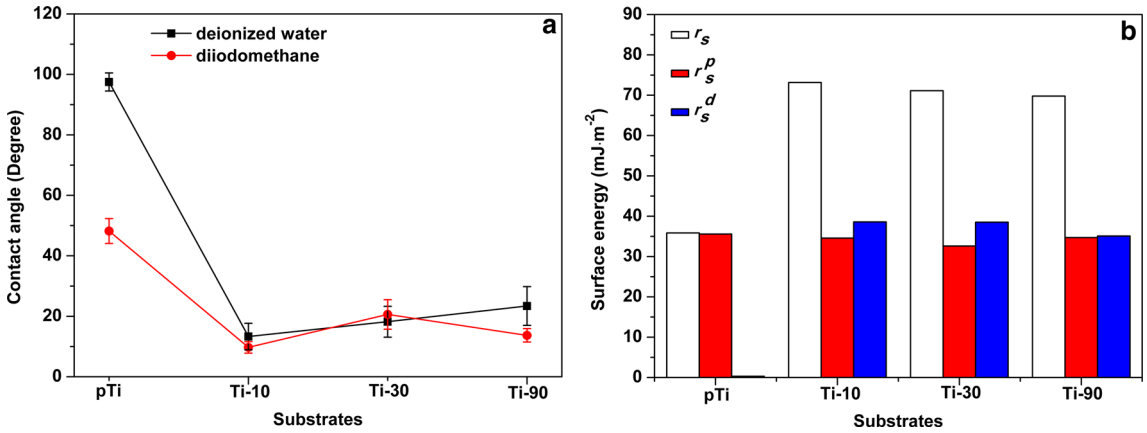

Fig. 3 Variation of contact angles (**a**) and surface energy component (**b**) of acid-etched titanium samples oxidized by H_2SO_4/H_2O_2 solution for various time: 0 min, 10 min, 30 min and 90 min

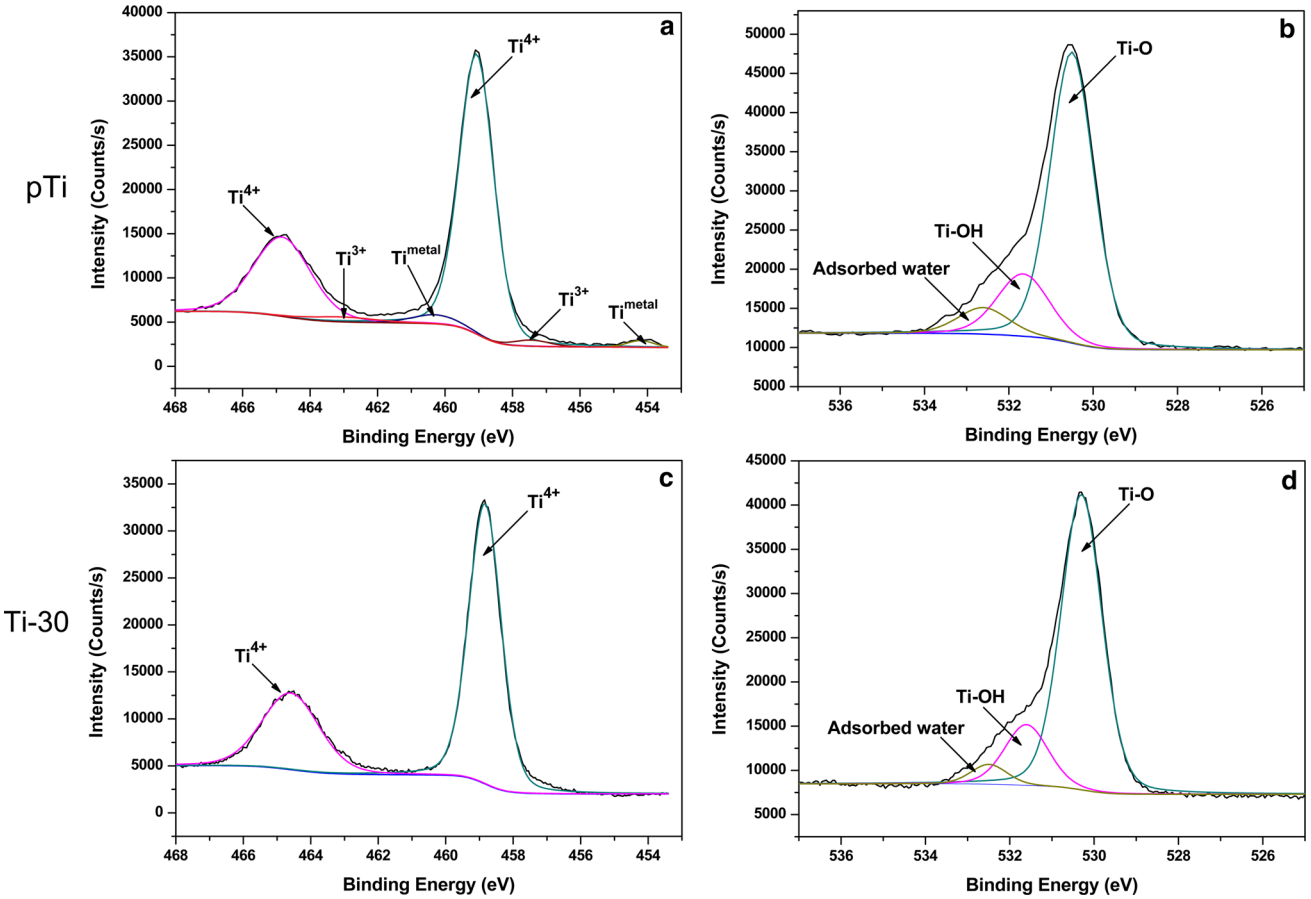

Fig. 4 High-resolution XPS spectra around Ti2p (**a**, **c**) and O1s (**b**, **d**) of pTi and Ti-30

oxidation itself can lead to the formation of crystallization of TiO_2. For example, poorly-crystallized anatase films were produced on titanium surface by Wu et al. [26] after soaking in 15 wt% H_2O_2 solution at 80 °C for 1 h. It is therefore possible for crystalline TiO_2 being obtained on titanium by elevating the reaction temperature found in our study.

3.4 Cell adhesion and proliferation assay

In order to verify that oxidative nanopatterning of titanium surface could improve the osseointegration of microrough titanium, titanium disks with a 30 min oxidation, set as a model, were tested for various biological capabilities in

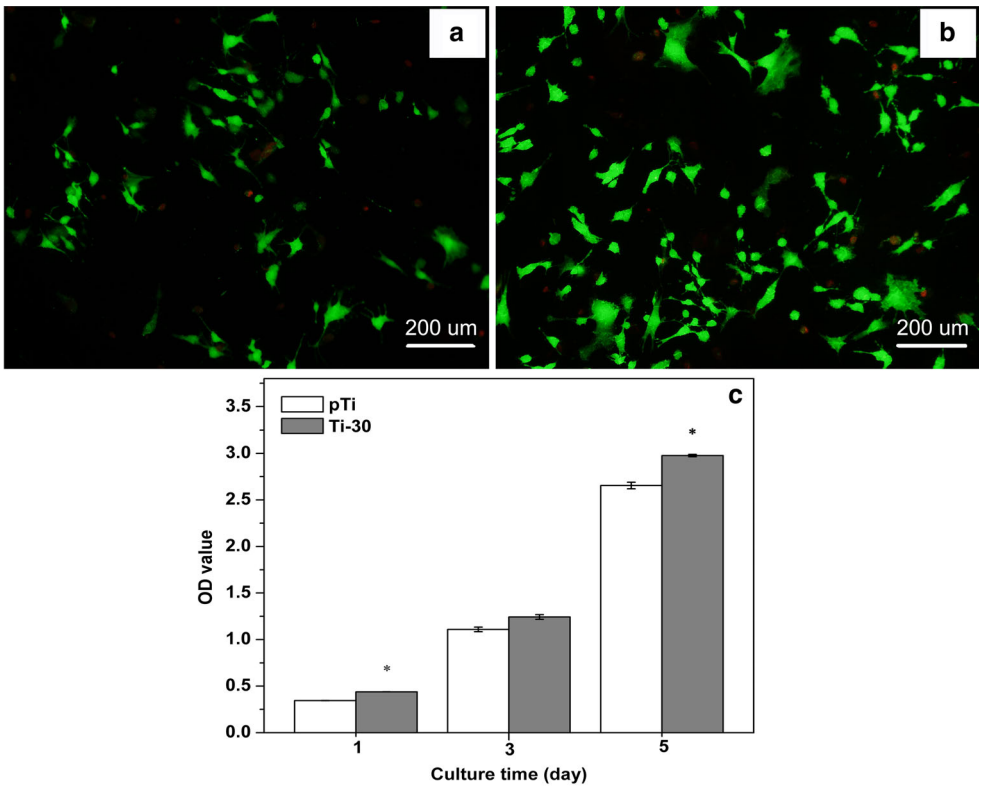

Fig. 5 Fluorescence micrographs (×100) of live/dead dye-stained murine BMSCs after 24 h of cultivation on pTi (**a**) and Ti-30 (**b**). Live cells appear *green* whilst dead cells are stained *red*. BMSCs proliferation measured using CCK-8 after incubation for 1, 3 and 5 days (**c**) ($n = 4$, $^*P < 0.05$ compared with pTi)

comparison with untreated acid-etched titanium disks. Initial cell adhesion, as an indicator of cytocompatibility, is an important phenomenon that sets the stage of migrate, proliferation, and differentiation. Therefore, it is required that cells firmly and quickly adhere to artificial implants. In the present study, cell adhesion was assessed using the live/dead kit. Fig. 5a and 5b shows fluorescent images of BMSCs after 24 h of culturing on the pTi and Ti-30 surfaces, respectively. In contrast, more viable cells were observed to attach on the Ti-30, which suggests a good affinity for nanostructured titanium oxide layer. Very few dead cells were present on both materials. Furthermore, closer inspection of cells on Ti-30 surfaces reveals a normal polygonal morphology, suggesting that cell spread was expedited remarkably on the nanopatterned surfaces. Higher adhesion on the surface does not necessarily suggest that the cells are viable and functional. Thus, the cell viability was assessed using the CCK-8 assay. The proliferation of BMSCs cells on micro-and micro/nano-textured Ti was investigated at days 1, 3 and 5 (Fig. 5c). BMSCs proliferation was observed to increase throughout the incubation period on both specimens. There was no significant difference after 3 days of culture between pTi and Ti-30. However, on the culture periods of 1 and 5 days, the cell numbers on pTi were remarkably lower ($p < 0.05$) than those on the Ti-30 samples. These results demonstrated the stimulatory effect of titania nanotextured layer on BMSCs adhesion and proliferation. Similar results were reported by [27]. One possible explanation is that the increased surface area created by nanopatterning might enhance protein adsorption [28], which then secondarily promotes initial adhesion of cells. Furthermore, BMSCs cells reportedly prefer hydrophilic surfaces rather than hydrophobic surfaces [29]. Thus, the combination of surface morphology and chemistry, which represents surface energy, might be responsible for the improved initial cell behavior.

3.5 Cell Morphology

Cells are inherently sensitive to their surrounding microenvironments, such as bio-chemical signals and surface topography of the materials [30]. It is generally accepted that cells use filopodia for spatial sensing in their movement and spread on structured surfaces. Figure. 6 shows the morphology of BMSCs cells on pTi and Ti-30 discs after culturing for 24 h. A greater number of initial adherent cells were observed on Ti-30 surfaces than on pTi samples (Fig. 6a,e). Besides, the BMSCs displayed dramatically different shapes related to the nanotopography of the substrate. Most cells on the pTi surface showed an elongated form and stretched less filopodia and cell bodies appeared to stand off the surface (Fig. 6b,c). Whereas, the cells attached on the Ti-30 were flattened and showed a

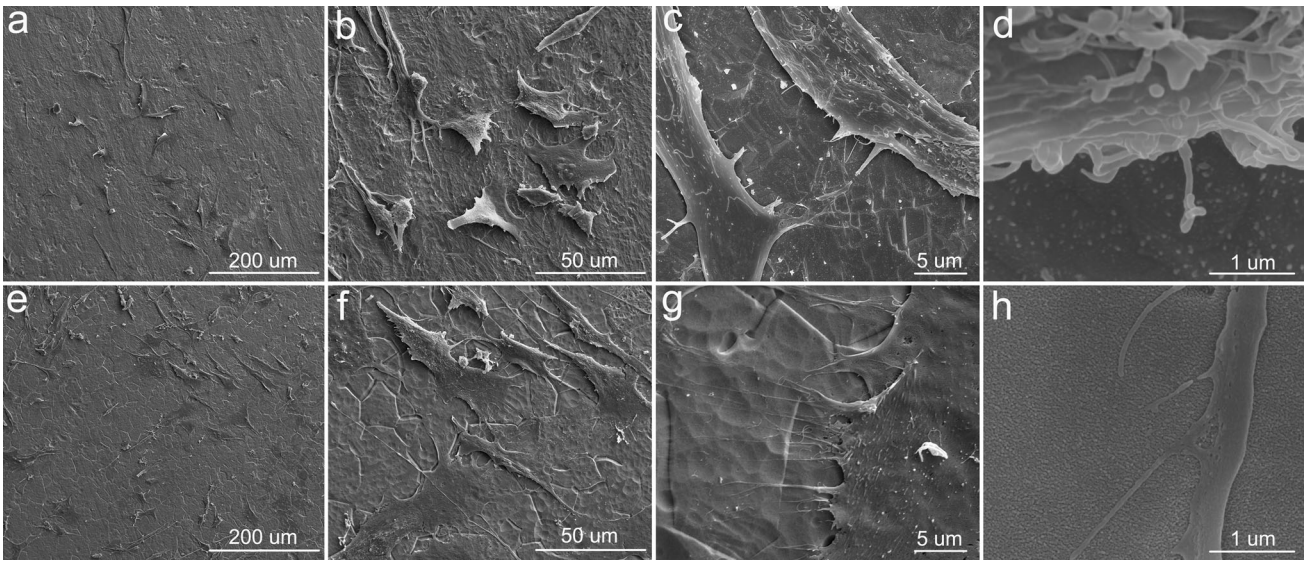

Fig. 6 SEM pictures showing the morphology of cells after 24 h of culture on pTi (**a–d**) and Ti-30 (**e–h**) samples. Pictures of a low magnification of ×200 (**a**, **e**) show the overall view. Pictures of ×2,000 (**b**, **f**) show the morphology of single cells and those of higher magnification (**c**, **g** , **d**, **h**) (×10,000, ×80,000) display the detail of cell interaction with the nanotextured layer

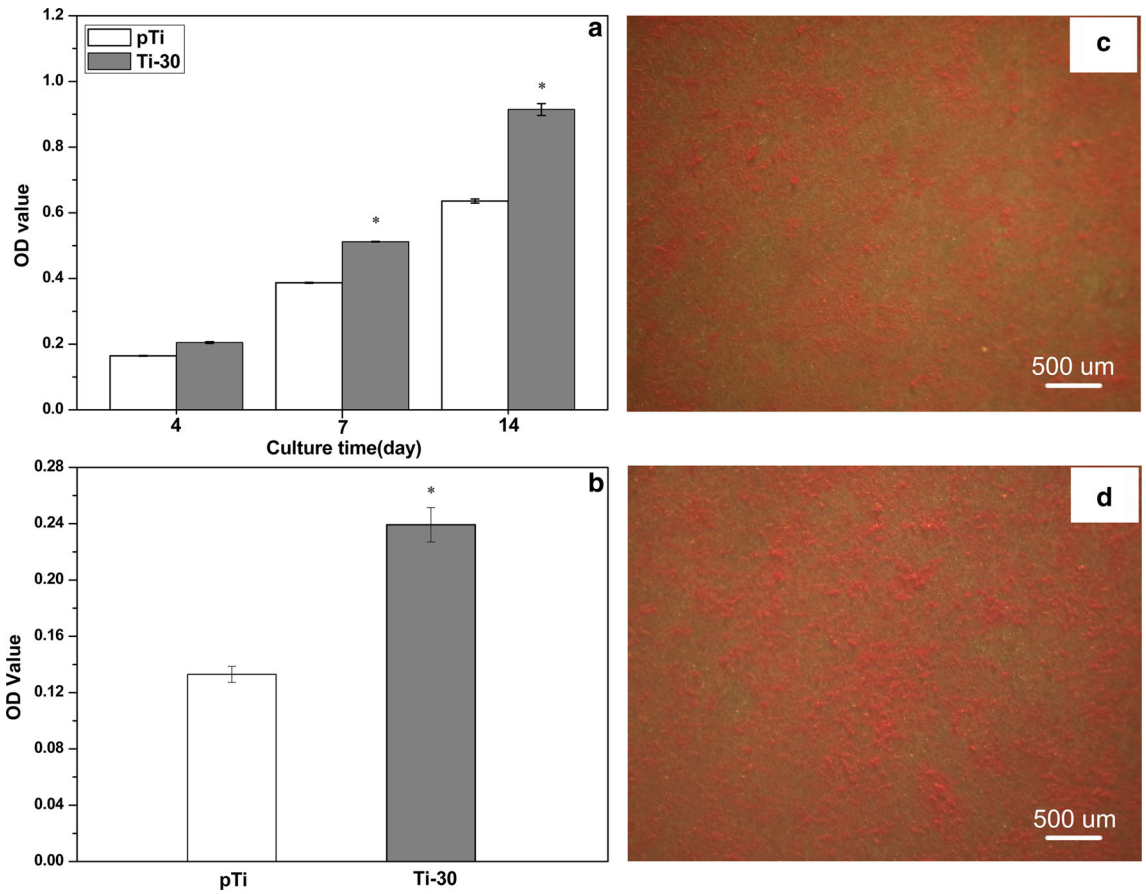

Fig. 7 ALP activity of BMSCs cells cultured on pTi and Ti-30 within different periods (**a**). Calcium deposition status of cells was assayed using colorimetrically quantitative analysis (**b**) ($n = 4$, $^*p < 0.05$ versus pTi group) and optical images stained with Alizarin Red for the pTi surface (**c**) and Ti-30 (**d**) after culturing for 14 days

polygonal shape with more filopodia (Fig. 6f). In addition, a great number of long and small diameter cytoplasmatic prolongations appeared on Ti-30 surface and spread in all directions (Fig. 6g). The higher magnification picture (Fig. 6h) discloses that the cellular filopodia tightly anchored to the nanostructured layer created by oxidative treatment, which was similar to results found in the literature [31]. The different cell adhesion morphologies demonstrated that addition of nanostructured titania layer to microrough titanium surface was beneficial for cell adhesion. The enhancement of cell adhesion on Ti-30 surface in the early stages (24 h) might be due to that nanofeature range not only facilitates formation of focal adhesions [32] but also contributes to provide anchorage for cells. Brammer et al. [33] reported that the nanotube layers could increase cell to cell interactions because of the nanoscale cues. In our results, spreading more filopodias on nanoneedle-structured surface seemed to exhibit the trend.

3.6 Osteogenic differentiation activity

The alkaline phosphatase and calcium deposition assays are commonly used to evaluate osteogenic differentiation in various cells. Quantitative results (Fig. 7a) at 4, 7 and 14 days confirmed that the cellular ALP activity increased with increasing culture time on both titanium discs. After 7 days of culture, BMSCs grown on Ti-30 substrates displayed significantly higher ($P = 0.004$) ALP activity than that on pTi surfaces. Mineralization of BMSCs was evaluated by alizarin red staining, a simple and convenient method for detecting calcium mineral deposition for assaying relative osteogenic differentiation. Fig. 7 (b–d) showed the semi-quantification and alizarin red staining for BMSCs cultured on the experimental surfaces after 14 days incubation. Significantly higher mineralization was detected in cells cultured on Ti-30 surfaces than the pTi groups. Taken together, these data indicated that osteogenic differentiation of BMSCs was accelerated on the nanostructured titanium substrates. Many authors have presented data showing the positive effects of nanopatterned surfaces on cell behavior, particularly related to osteogenesis [34, 35]. Besides surface topography, surface chemistry and wettability also play a vital role in regulating cell behavior. However, it is difficult to distinguish the effect of these individual surface properties on cell response since they are directly connected. As to the detailed mechanisms of the promoting effect of nanofeatures on BMSCs differentiation on titanium surface, further studies are needed.

4 Conclusions

This study has established the feasibility of creating titania nanostructured films on microrough titanium surfaces by chemical oxidation to enhance their biological properties without significantly altering their surface morphology. The nanostructured layers obtained by oxidation could be well controlled by the adjustment of duration time. An increase in the attachment, spreading behavior, proliferation, and differentiation of BMSCs was observed on micro–nano textured titanium oxidized surfaces. Therefore, this oxidative nanofunctionalization of microtopographical titanium has potential as an effective way to improve bone-titanium integration in vivo.

Acknowledgments We gratefully acknowledge the financial support of National Key Basic Research Program of China (Grant No. 2012CB619100), the National Natural Science Foundation of China (Grant No. 51372081, 51072055, 81271957) and special funding for university talent introduction of Guangdong Province (GX N).

References

1. Liu X, Chu P, Ding C. Surface modification of titanium, titanium alloys, and related materials for biomedical applications. Mater Sci Eng. 2004;47(3–4):49–121.
2. Karthega M, Nagarajan S, Rajendran N. In vitro studies of hydrogen peroxide treated titanium for biomedical applications. Electrochim Acta. 2010;55(6):2201–9.
3. Wu JM, Wang M, Li YW, Zhao FD, Ding XJ, Osaka A. Crystallization of amorphous titania gel by hot water aging and induction of in vitro apatite formation by crystallized titania. Surf Coat Technol. 2006;201(3):755–61.
4. Lavenus S, Trichet V, Le Chevalier S, Hoornaert A, Louarn G, Layrolle P. Cell differentiation and osseointegration influenced by nanoscale anodized titanium surfaces. Nanomedicine. 2012;7(7):1045–66.
5. Dalby MJ, Gadegaard N, Wilkinson CD. The response of fibroblasts to hexagonal nanotopography fabricated by electron beam lithography. J Biomed Mater Res A. 2008;84(4):973–9.
6. Rani VD, Manzoor K, Menon D, Selvamurugan N, Nair SV. The design of novel nanostructures on titanium by solution chemistry for an improved osteoblast response. Nanotechnology. 2009;20(19):195101.
7. Zhang W, Li Z, Liu Y, Ye D, Li J, Xu L, et al. Biofunctionalization of a titanium surface with a nano-sawtooth structure regulates the behavior of rat bone marrow mesenchymal stem cells. Int J Nanomed. 2012;7:4459–72.
8. Yang W, Xi X, Shen X, Liu P, Hu Y, Cai K. Titania nanotubes dimensions-dependent protein adsorption and its effect on the growth of osteoblasts. J Biomed Mater Res A. 2013.
9. Zhao L, Mei S, Chu PK, Zhang Y, Wu Z. The influence of hierarchical hybrid micro/nano-textured titanium surface with titania nanotubes on osteoblast functions. Biomaterials. 2010;31(19):5072–82.
10. Ueno T, Tsukimura N, Yamada M, Ogawa T. Enhanced bone-integration capability of alkali- and heat-treated nanopolymorphic titanium in micro-to-nanoscale hierarchy. Biomaterials. 2011;32(30):7297–308.
11. de Oliveira P Tambasco, Nanci A. Nanotexturing of titanium-based surfaces upregulates expression of bone sialoprotein and osteopontin by cultured osteogenic cells. Biomaterials. 2004;25(3):403–13.
12. Vetrone F, Variola F, de Oliveira P Tambasco, Zalzal SF, Yi JH, Sam J, et al. Nanoscale oxidative patterning of metallic surfaces to modulate cell activity and fate. Nano Lett. 2009;9(2):659–65.

13. Variola F, Lauria A, Nanci A, Rosei F. Influence of treatment conditions on the chemical oxidative activity of H_2SO_4/H_2O_2 mixtures for modulating the topography of titanium. Adv Eng Mater. 2009;11(12):B227–34.
14. Variola F, Yi JH, Richert L, Wuest JD, Rosei F, Nanci A. Tailoring the surface properties of Ti_6Al_4 V by controlled chemical oxidation. Biomaterials. 2008;29(10):1285–98.
15. Yi JH, Bernard C, Variola F, Zalzal SF, Wuest JD, Rosei F, et al. Characterization of a bioactive nanotextured surface created by controlled chemical oxidation of titanium. Surf Sci. 2006;600:9.
16. Deyneka-Dupriez N, Kocdemir B, Herr U, Fecht HJ, Wilke HJ, Claes L. Interfacial shear strength of titanium implants in bone is significantly improved by surface topographies with high pit density and microroughness. J Biomed Mater Res B. 2007;82(2):305–12.
17. Rani VV, Vinoth-Kumar L, Anitha VC, Manzoor K, Deepthy M, Shantikumar VN. Osteointegration of titanium implant is sensitive to specific nanostructure morphology. Acta Biomater. 2012;8(5):1976–89.
18. Ranella A, Barberoglou M, Bakogianni S, Fotakis C, Stratakis E. Tuning cell adhesion by controlling the roughness and wettability of 3D micro/nano silicon structures. Acta Biomater. 2010;6(7):2711–20.
19. Wei J, Igarashi T, Okumori N, Igarashi T, Maetani T, Liu B, et al. Influence of surface wettability on competitive protein adsorption and initial attachment of osteoblasts. Biomed Mater. 2009;4(4):045002.
20. Serro A, Saramago B. Influence of sterilization on the mineralization of titanium implants induced by incubation in various biological model fluids. Biomaterials. 2003;24(26):4749–60.
21. Pegueroles M, Aparicio C, Bosio M, Engel E, Gil FJ, Planell JA, et al. Spatial organization of osteoblast fibronectin matrix on titanium surfaces: effects of roughness, chemical heterogeneity and surface energy. Acta Biomater. 2010;6(1):291–301.
22. Michiardi A, Aparicio C, Ratner BD, Planell JA, Gil J. The influence of surface energy on competitive protein adsorption on oxidized NiTi surfaces. Biomaterials. 2007;28(4):586–94.
23. Anselme K, Bigerelle M, Ponche A. Relative influence of surface topography and surface chemistry on cell response to bone implant materials. Part 1: physico-chemical effects. Proc Inst Mech Eng. 2010;224(12):1471–86.
24. Espinar E, Llamas JM, Michiardi A, Ginebra MP, Gil FJ. Reduction of Ni release and improvement of the friction behaviour of NiTi orthodontic archwires by oxidation treatments. J Mater Sci Mater Med. 2011;22(5):1119–25.
25. He J, Zhou W, Zhou X, Zhong X, Zhang X, Wan P, et al. The anatase phase of nanotopography titania plays an important role on osteoblast cell morphology and proliferation. J Mater Sci Mater Med. 2008;19(11):3465–72.
26. Wu JM, Hayakawa S, Tsure K, Osaka A. Porous titania films prepared from interactions of titanium with hydrogen peroxide solution.pdf. Scr Mater. 2004;46:6.
27. Chen X, Cai K, Lai M, Zhao L, Tang L. Mesenchymal stem cells differentiation on hierarchically micro/nano-structured titanium substrates. Adv Eng Mater. 2012;14(5):B216–23.
28. Lord MS, Foss M, Besenbacher F. Influence of nanoscale surface topography on protein adsorption and cellular response. Nano Today. 2010;5(1):66–78.
29. Shin YN, Kim BS, Ahn HH, Lee JH, Kim KS, Lee JY, et al. Adhesion comparison of human bone marrow stem cells on a gradient wettable surface prepared by corona treatment. Appl Surf Sci. 2008;255(2):293–6.
30. Patel S, Kurpinski K, Quigley R, Gao H, Hsiao BS, Poo MM, et al. Bioactive nanofibers: synergistic effects of nanotopography and chemical signaling on cell guidance. Nano Lett. 2007;7(7):2122–8.
31. Mendonca G, Mendonca DB, Aragao FJ, Cooper LF. The combination of micron and nanotopography by H(2)SO(4)/H(2)O(2) treatment and its effects on osteoblast-specific gene expression of hMSCs. J Biomed Mater Res A. 2010;94(1):169–79.
32. Biggs MJ, Richards RG, Dalby MJ. Nanotopographical modification: a regulator of cellular function through focal adhesions. Nanomedicine. 2010;6(5):619–33.
33. Brammer KS, Oh S, Cobb CJ, Bjursten LM, van der Heyde H, Jin S. Improved bone-forming functionality on diameter-controlled TiO(2) nanotube surface. Acta Biomater. 2009;5(8):3215–23.
34. de Oliveira PT, Zalzal SF, Beloti MM, Rosa AL, Nanci A. Enhancement of in vitro osteogenesis on titanium by chemically produced nanotopography. J Biomed Mater Res A. 2007;80(3):554–64.
35. Kaur G, Valarmathi MT, Potts JD, Jabbari E, Sabo-Attwood T, Wang Q. Regulation of osteogenic differentiation of rat bone marrow stromal cells on 2D nanorod substrates. Biomaterials. 2010;31(7):1732–41.